



Title	Dynamic Mixing Experiment for Oxide Film Formation with ECR Ion Beam(Physics, Process, Instrument & Measurement)
Author(s)	Miyake, Shoji; Honda, Kazuhiko; Satou, Mamoru et al.
Citation	Transactions of JWRI. 1991, 20(1), p. 27-33
Version Type	VoR
URL	<a href="https://doi.org/10.18910/10752">https://doi.org/10.18910/10752</a>
rights	
Note	

*The University of Osaka Institutional Knowledge Archive : OUKA*

<https://ir.library.osaka-u.ac.jp/>

The University of Osaka

# Dynamic Mixing Experiment for Oxide Film Formation with ECR Ion Beam<sup>†</sup>

Shoji MIYAKE\*, Kazuhiko HONDA\*\*, Mamoru SATOU\*\*\* and Bunkei KYOU\*\*\*\*

## Abstract

A compact dynamic mixing system equipped with a bucket type ECR ion source was developed for the formation of oxide films. The machine characteristics was tested and modified to be appropriate for the mixing experiment. The ion energy can be varied between 5 to 25keV with sufficient current density for the oxide film synthesis. Formation of titanium oxide films were performed by the combination of electron beam evaporation of Ti metals and oxygen ion beam injection onto Si wafers and/or quartz plates. Only rutile type  $TiO_2$  films were obtained by varying the beam energy and the arrive rate of Ti/O.

**KEY WORDS:** (Oxide Film) (Titania) (Dynamis Mixing) (Ion Beam) (ECR Ion Source)

## 1. Introduction

Among various ion beam methods for material modification, dynamic mixing method<sup>1)</sup> has increasingly attracted attention as one of the key technologies to obtain new surfaces with complex, layered or gradient structures and with strong adhesion between base materials. Experimental studies on dynamic mixing have so far been devoted mainly to the formation of nitride films<sup>2-5)</sup>. As for oxide films only the formation of ITO (Indium Tin Oxide)<sup>6)</sup> and of  $TiO_7$  films were reported.

In our previous report<sup>7)</sup> of  $TiO$  synthesis, we were not able to obtain  $TiO_2$  films even if we changed various external parameters. We considered that the main cause of not obtaining  $TiO_2$  films came from the shortage of oxygen ion supply. In that experiment a cold cathode discharge type ion source was used, and the ion dose obtainable was in the range below  $1 \times 10^{17}/cm^2$ .

To overcome this problem we applied a bucket type ECR ion source<sup>8)</sup> with a permanent magnet assembly and developed a compact dynamic mixing system for oxide and/or nitride thin film formation. With this system we could obtain the oxygen ion beam current higher than 1mA with a moderately uniform distribution of the beam in the radial direction.

In the dynamic mixing of titanium oxide films we could successfully obtain rutile type  $TiO_2$  films as expected. This

report describes experimental results on the performance of the dynamic mixing system with an ECR ion source and the property of titanium oxide films prepared by changing various external parameters.

## 2. Experimental apparatus and methods

Figure 1 shows a schematic diagram of the experimental apparatus. Oxygen or other gas ion beams (10) from an ECR bucket-type ion source (1) are horizontally injected onto the sample holder (8) in the mixing chamber. The

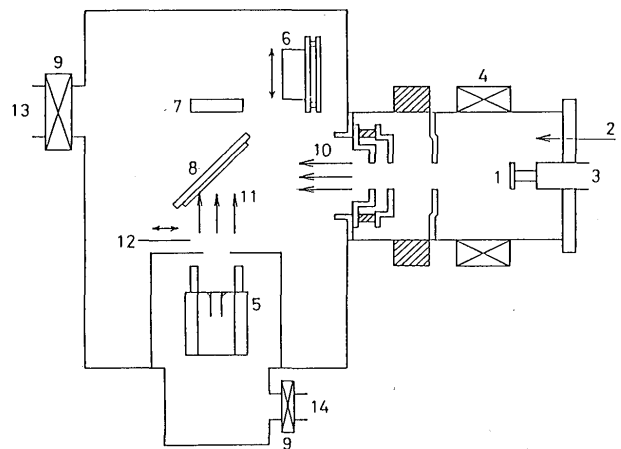


Fig. 1 Schematic diagram of experimental apparatus.

† Received on May 7, 1991.

\* Professor

\*\* Nippon Steel Corporation

\*\*\* Chief Senior Researcher, Government Industrial Research Institute, Osaka

\*\*\*\* Professor, Kinki University

Transactions of JWRI is published by Welding Research Institute of Osaka University, Ibaraki, Osaka 567, Japan

distance between the source and the holder is about 20cm, and the sample holder is made of Cu with a dimension of 50mm diameter and 30mm thickness. It can be rotated with a maximum rate of 100rpm and the angle between the direction of the beam injection and the surface normal of the holder is kept to be 45 degrees.

The mixing chamber and the ion source is electrically insulated. In the ion source various rare and molecular gas plasmas can be produced by the microwave energy of  $f = 2.45\text{GHz}$  fed through a coaxial antenna (3) with the maximum power input of 500W. A hexapole cusp magnetic field is arranged by SmCo permanent magnets (4) set along the SUS discharge chamber wall, with which the ECR field of 875G is obtained near the wall within the chamber.

Ions are extracted and accelerated through a 3-electrode system with an energy ranging from 1 to 30keV. The first (extraction and acceleration) electrode is set to be a potential that is the same with the discharge chamber wall, where a positive high voltage is applied for accelerating ions to a desired value. The second (accel/decel, A/D) electrode is biased negatively to the earth potential to suppress the electron backflow to the antenna (3) and to make an appropriate beam extraction characteristics. The third (ground) electrode is kept to be the earth potential and is connected to the mixing chamber.

The beam extracted from the ground electrode is limited by a SUS plate with a hole of 30mm diameter, which is not shown in the figure, and the total current of the beam is measured with a Faraday cup (6) which acts also as a beam shutter.

Metal vapours (11) simultaneously deposited onto the sample during the beam injection are supplied from below by a 2kW EB (electron beam) evaporator (5). The electron beam energy is fixed to be 4keV and the emission current can be varied up to 500mA. The film thickness is monitored during the dynamic mixing with a thickness monitor (7). The distance between the holder and the evaporator or the thickness monitor is about 20cm.

The mixing chamber is evacuated mainly by a cryopump (13) of 1500l/s through a valve (9). The base pressure in the chamber reached to  $9 \times 10^{-5}\text{Pa}$ . During the mixing the pressure was kept to be  $3.0 \times 10^{-3}\text{Pa}$ . In the area of the EB evaporator, a 50l/s turbomolecular pump is additionally used to perform differential pumping and to guarantee the stable operation of evaporation during the mixing.

Characterization of titanium oxide films prepared were made with XRD, RBS, XPS, Raman Spectroscopy, UV-Visible absorption and FTIR methods. The resistivity of the film was measured by Van der Pauw method. In this report data by XRD and RBS will be discussed below.

### 3. Results and Discussion

#### 3.1 Machine characteristics

The bucket type ECR ion source applied in this machine is operated at a pressure in the range of  $10^{-4}\text{Pa}$  within the discharge chamber<sup>8)</sup> and the source is directly coupled to the mixing chamber, by which the background pressure is increased during the operation of the ion beam.

In our original design, evacuation of the system was performed with a turbomolecular pump of 500l/s and there was no casing around the EB evaporator. The base pressure obtained without ECR plasma operation and EB evaporation was  $2.7 \times 10^{-4}\text{Pa}$ . When the hole size of the extraction electrodes was 10mm, an oxygen beam having a total current higher than 1mA was obtained easily at a beam energy of 10keV, and the background pressure during mixing was kept to be about  $5 \times 10^{-3}\text{Pa}$ . The beam profile, however, was nonuniform and films prepared had a strong inhomogeneity in its outlook as well as in their property.

We changed the diameter of the electrodes to 25mm and a moderately uniform beam was obtained with the total current higher than 3mA at an extraction voltage  $V_{ext}$  of 10kV, whose result is shown in Fig. 2. In the figure the oxygen flow rate is 1.4sccm and the background pressure increases to about  $1.8 \times 10^{-2}\text{Pa}$ . The input microwave is 200W and the voltage  $V_{A/D}$  on the A/D electrode is  $-2.0\text{kV}$ .

When Ti metal was evaporated in this condition, a stable operaeration of the plasma became impossible, as the

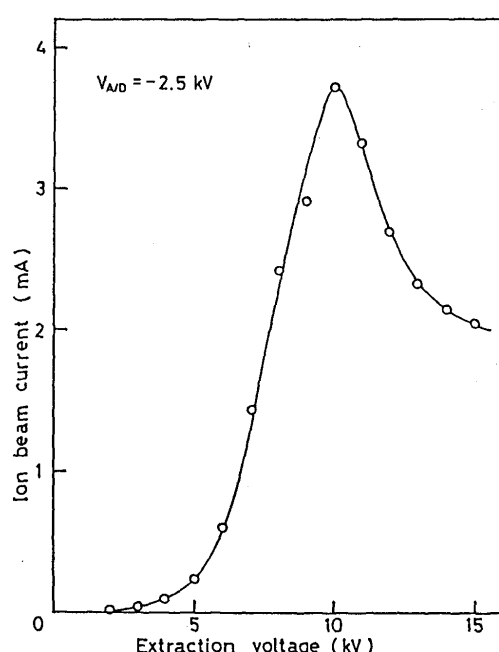


Fig. 2 Ion beam current versus extraction voltage in the case of 25mm<sup>2</sup> single hole electrodes

pressure in the mixing and discharge chambers varied rapidly due to the gettering action of evaporated Ti metal. The operation of the evaporator was not also stable.

To overcome these difficulties we changed the turbomolecular pump by a cryopump of 1500l/s, and the extraction electrodes of 25mm<sup>2</sup> single hole to 30mm<sup>2</sup> multi-aperture type made of carbon plates. The diameter of each aperture is 2mm. Moreover the differential pumping was given with a casing around the evaporator by a 50l/s turbomolecular pump. With this modified system we could obtain the base pressure of  $9 \times 10^{-5}$ Pa without the operation of the ion source and the evaporator as stated in the former section.

**Figure 3** shows the background pressure in the mixing chamber without Ti evaporation as a function of the oxygen gas flow rate into the ECR discharge chamber. Triangles show the data of the 25mm<sup>2</sup> hole electrodes and circles that of 30mm<sup>2</sup> multi-aperture ones. In the case of the former electrodes the pressure becomes a little higher and the discharge can not be sustained at a gas flow rate lower than 3.3sccm. While in the latter case the ECR plasma is obtained stably even below 1.0 sccm, and the gas pressure can be kept to be low at about  $5.0 \times 10^{-3}$ Pa.

When the evaporation of Ti atoms is performed simultaneously, the pressure in the mixing chamber is lowered to a value of  $3.0 \times 10^{-3}$ Pa as described already, even in the case of the multi-aperture electrodes. The system, however, induces no change on the beam operation as well as on the vapour deposition, by which we can successfully perform the dynamic mixing experiments.

With the above mentioned modification we measured the total ion beam current of oxygen as a function of the extraction voltage. **Figure 4** gives an example where the

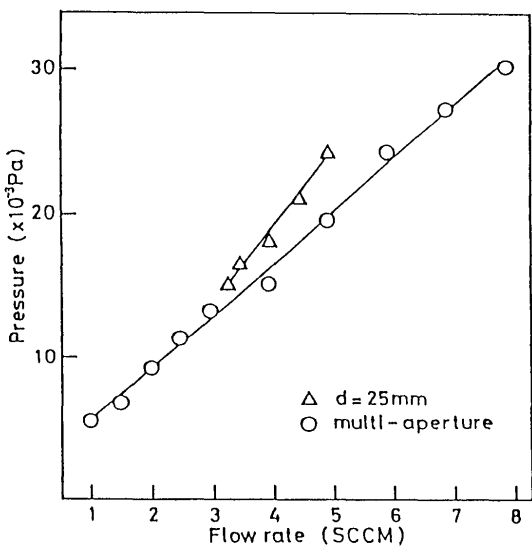


**Fig. 3** Variation of background pressure with oxygen flow rate.

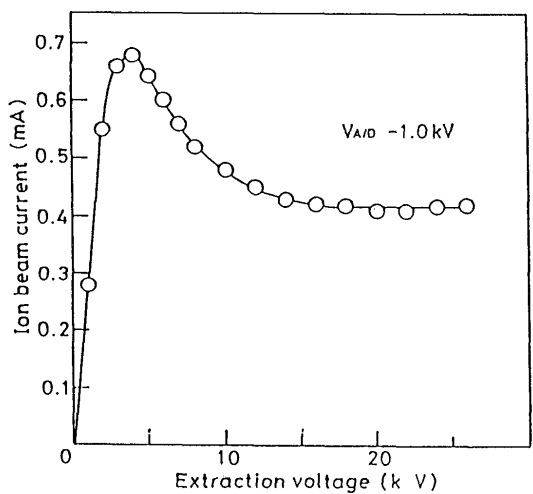


**Fig. 4** Ion beam current versus extraction voltage in the case of 30mm<sup>2</sup> multi-aperture electrodes.

oxygen flow rate is 0.7 sccm and the votabe  $V_{A/D}$  on the A/D electrode is kept to be  $-1.0$ kV. The microwave power input is 500W. We find a similar curve with that of Fig. 2 but the total current is not higher than 1mA mainly because of the lack of the microwave power input more than 500W. The saturation and decrease of the current at a high energy will come from the change of the beam optics bringing the beam loss to the A/D or ground electrode. Nevertheless the current obtained was sufficient to perform the mixing experiments, as we found that a current higher than 1mA induced a severe sputtering of Si wafers in the ion energy of 5 to 25keV under consideration by which the film formation was difficult.

**Figure 5** is an example of the radial beam profile measured by a plane tungsten probe set at 5cm apart from the sample along the beam path, the probe dimension is 2mm in diameter. The beam shows a Gaussian profile with a full width of half maximum (FWHM) of about 15mm irrespective of the variation of  $V_{EXT}$ . By increasing  $V_{A/D}$  the profile indicated a stronger inhomogeneity. To improve the

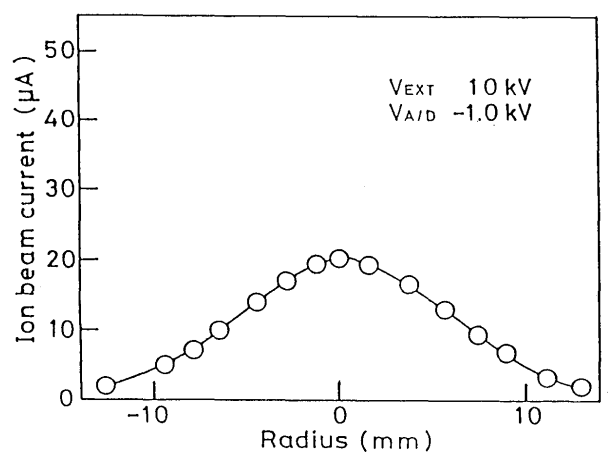


**Fig. 5** Radial beam profile at  $V_{EXT} = 10$ kV and  $V_{A/D} = -1$ kV.

beam optics for obtaining a more uniform beam profile further experiments are necessary by changing the dimensional parameters of the electrode system.

As for the ion species included in the total ion current in this source, it was reported<sup>8)</sup> that the ratio of  $O_2^+$  to  $O^+$  ion current was 2 to 1 in the typical operating condition.

Ion beam technologies are considered to be one of the low temperature process which enables us obtain various new phases of material modification. The injected ion beams, however, have a high energy and the power input to the sample can be large as several 10W when the beam current reaches to about 1mA. As the thermal conductivity of Si wafers or quartz plates are not good, the substrate temperature may be increased considerably when the holder is not cooled well. We measured the time variation of the surface temperature of a Si wafer on the side of the beam injection with a thermocouple. The result is shown in Fig. 6. The oxygen beam current is fixed to be  $500\mu A$  and the gas flow rate is 0.7sccm. The deposition of Ti vapours is not given. The substrate temperature increases rapidly and saturates to nearly a constant value within several minutes from the start of the beam injection. The saturated temperature changes with the beam energy and is around 500K. This value is low enough when we compare the

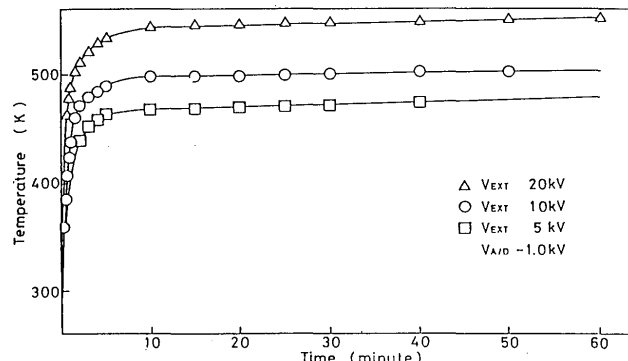


Fig. 6 Time variation of substrate temperature for various  $V_{EXT}$ .

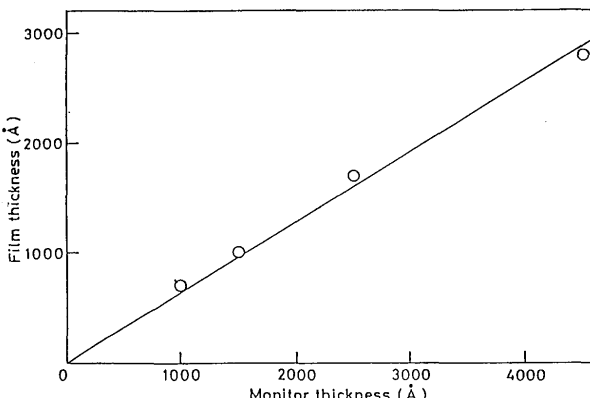


Fig. 7 Film thickness compared with that by the thickness monitor.

formation of  $TiO_2$  films in other methods typically at a temperature higher than 800K.

We checked the performance of the thickness monitor by evaporating Ti metals onto the sample and the monitor. The result is shown in Fig. 7. The actual film thickness on the Si wafers are measured with a Talystep. The thickness by the Talystep indicates a value of  $1/\sqrt{2}$  of the one by the monitor. This is because the vapour of Ti particles impinges onto the sample with an angle of 45 degrees to the surface normal. To avoid the nonuniform film synthesis over the surface, the holder was rotated and the film thickness could be kept to be uniform over the area of 25mm in radius.

### 3.2 $TiO_2$ film synthesis

Typical experimental conditions for the  $TiO_2$  film formation by the dynamic mixing are shown in Table 1. Si wafers used as a substrate are (100) single crystals and carbon plates are used in the analysis of RBS data to separate the peaks of Ti and O atoms in the data more clearly than the case of Si wafers. Quartz plates are used for the analysis of optical property.

The oxygen ion dose is calculated from the ion current density and the mixing time assuming the ratio of  $O_2^+ / O^+$  to be 2.0. The Ti dose is deduced from the data in Fig. 7 and the ion current is fixed to be  $500\mu A$ . The arrival rate  $Ti/O$  of Ti atoms and effective  $O^+$  ions from the beam onto the sample is varied by changing the Ti deposition rate. The prepared films were 1000–3000Å in thickness and the range of implanted oxygen ions is around 100Å at an energy of 10keV, which is sufficiently low in comparison with the film thickness but high enough for obtaining strong

Table 1 Typical experimental conditions of  $TiO_2$  film synthesis.

Substrate	Si (100) wafer, Carbon, Quarts plate
$O^+$ ion dose	$0.7 \sim 1.6 \times 10^{18} \text{ ions/cm}^2$ ( $O_2^+ / O^+ = 2$ )
Ti deposition rate	$1.5 \sim 4.0 \text{ Å/s}$
Pressure	$9.0 \times 10^{-5} \text{ Pa (base)}$ $3.0 \times 10^{-3} \text{ Pa (operation)}$
Beam diameter	30mm
Ion-energy	3 ~ 25 keV
Beam current	0.5 mA (10 keV)
Substrate temperature	470 ~ 530 K
Film thickness	1000 ~ 3000 Å

adhesion of the film with substrates.

First synthesis of titanium oxide films was performed by varying the ion beam energy and prepared films were analyzed by XRD, whose result is shown in Fig. 8. In this figure the arrival rate  $Ti/O$  is kept to be nearly the same for all data. It is clear that they indicate the formation of only rutile type  $TiO_2$  films. In other methods such as electron beam deposition, ion plating, RF sputtering, reactive evaporation, ion beam sputtering and ion assisted deposition (IAD), fabricated  $TiO_2$  films almost have amorphous or anatase structure<sup>9-11</sup>. In the ion cluster beam (ICB) method rutile  $TiO_2$  films are obtained<sup>12</sup> in a limited condition. In a different experiment<sup>13</sup> of 150keV oxygen

ion implantation on the Ti substrate, it reveals the formation of rutile  $TiO_2$  surface at room temperature when the ion dose exceeded  $1 \times 10^{18}/cm^2$ .

Another interesting feature in Fig. 8 is the growth of (110) plane of  $TiO_2$  crystal by an increase of the ion energy. Peak intensity of other planes does not show remarkable variation. The reason of this growth in a specific plane of the crystal is not clear at present, but we consider that it is not brought by an increase in the substrate temperature during the mixing. As we find in Fig. 6, the substrate temperature changes from 470K to 530K when the beam energy is varied from 5 to 20keV, which is sufficiently low in comparison with other methods.

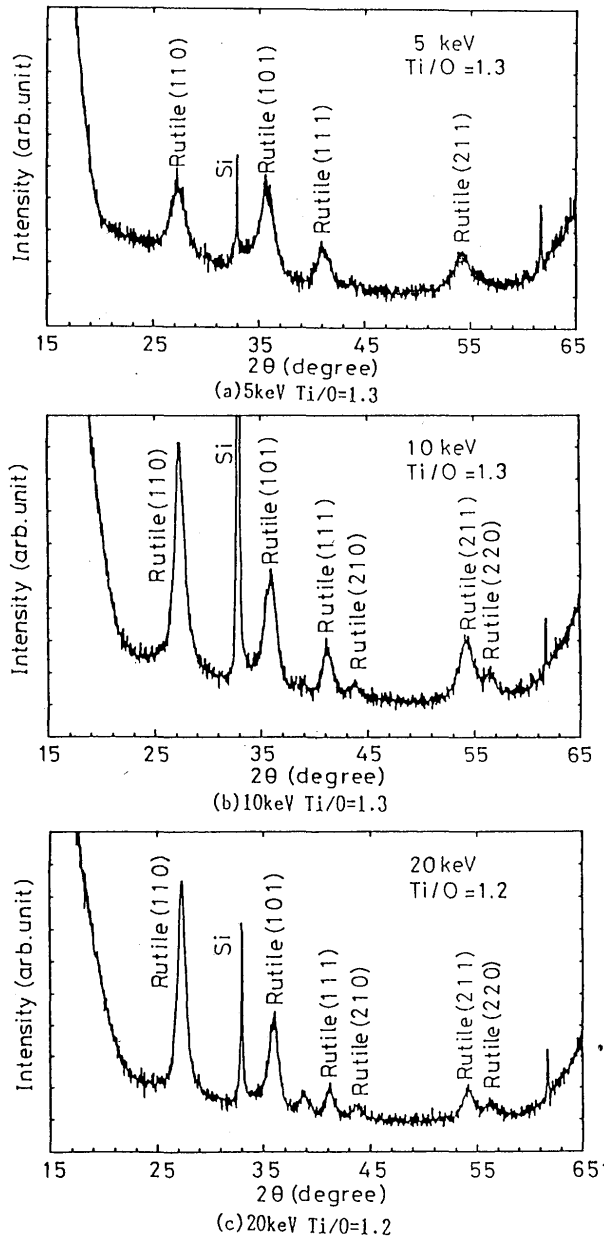


Fig. 8 XRD data of  $TiO_2$  films for various beam energies

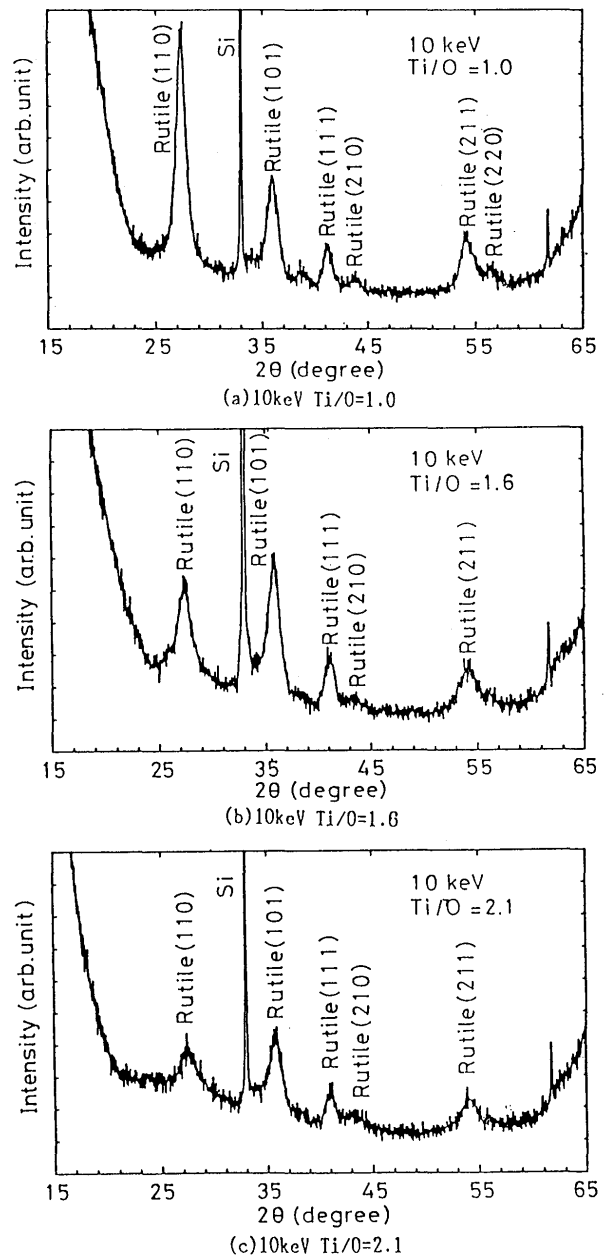


Fig. 9 XRD data for various arrival rates  $Ti/O$ .

To test this property further, we fabricated films for various arrival rates  $Ti/O$  by keeping the ion energy at 10keV. The result is shown in **Fig. 9**. Again we find the formation of rutile type  $TiO_2$ , and the growth of (110) plane is observed when the arrival rate is decreased. Indeed the variation of Ti deposition rate induces quite little change of the substrate temperature and the temperature will be about 500K for all data in this figure. So that we may conclude that the growth in a specific plane of the crystal with ion beam injection is not brought by the temperature effect but by a unique ion induced crystallization which is observed also in other materials.

We further checked the film structure without injecting the ion beam and found no peak in XRD other than Si line that is also found in Figs. 8 and 9.

Next we studied the composition of prepared  $TiO_2$  films by RBS method. In obtaining RBS data we applied a carbon plate as the substrate to observe peaks of Ti and O more clearly than the case of a Si wafer. When the ion beam was injected, we deposited Au vapour on the carbon plate beforehand to avoid the inclusion of carbon into the film by high energy ions. The result is shown in **Fig. 10**.

In this figure data without ion injection as well as without plasma are also given where Au deposition is not given. We aimed at knowing the influence of the residual oxygen atoms or molecules in the mixing chamber to the film composition, even when the ion injection was not performed. In all charts the spectrum of Ti from 1.1MeV and that of O from 0.55 MeV are observed clearly. The peak observed around 1.25MeV corresponds to Au. The background pressure of the mixing chamber is  $2.6 \times 10^{-3}$ Pa for all cases.

The composition ratio of Ti and O in the film was calculated from these data. In the case of Ti deposition with only the oxygen flow,  $Ti/O$  was 1:2.2. When the ECR plasma was operated without the ion injection, the ratio was 1:1.9 and in the condition of the mixing it gave 1:1.9. Other data of the mixing obtained by varying  $V_{ext}$  or  $Ti/O$  also indicated  $Ti/O = 1:1.7 - 2.0$ . Indeed all films have nearly the stoicometric composition. We note that the ion dose gives quite little influence to the film composition and the oxygen inflow from the source region into the mixing chamber has an essential effect, as titanium is quite reactive with oxygen and easy to form various solid solutions.

We conclude that the base pressure of  $2.6 \times 10^{-3}$ Pa is sufficiently high for the appearance of the reactive process between Ti and  $O_2$  molecules on the surface of the film, by which control of the background pressure is quite important in the dynamic mixing process of oxides as well as nitrides. Further experiments on this problem are under way and the result will be published in a separate paper.

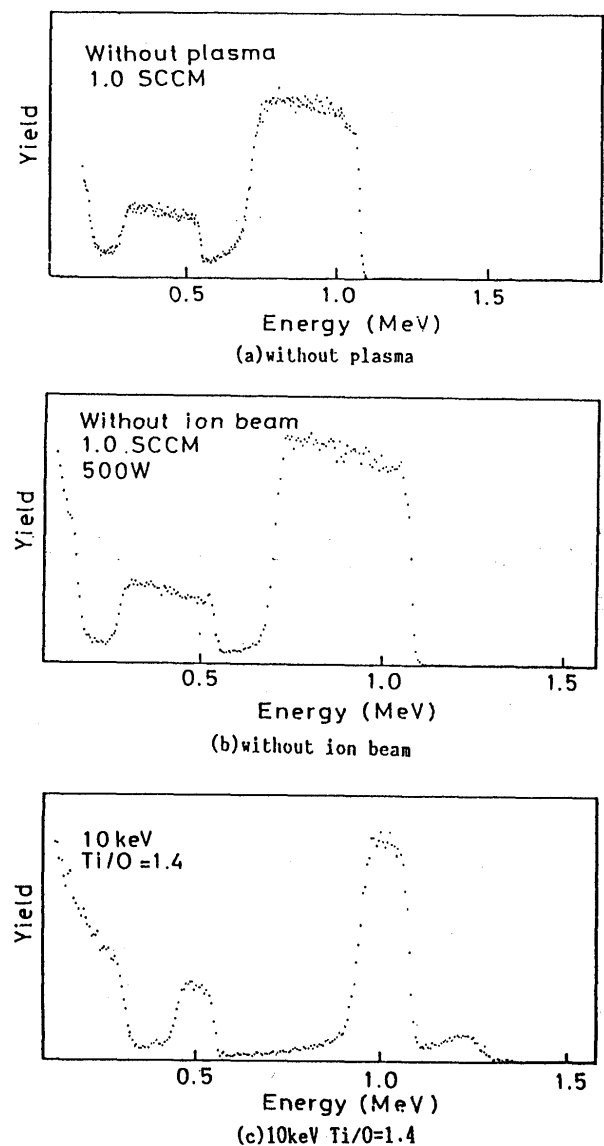


Fig. 10 RBS data in different conditions of Ti evaporation.

#### 4. Conclusion

A compact dynamic mixing system equipped with an ECR ion source was developed for obtaining various oxide and/or nitride films. With this source a high current oxygen ion beam sufficient for the oxide formation was obtained quite easily. The system characteristics of the machine was tested and modified for obtaining appropriate conditions of the mixing experiment.

An oxygen ion beam giving the ion dose higher than  $1 \times 10^{18}/cm^2$  was obtained keeping the base pressure of the mixing chamber at about  $5.0 \times 10^{-3}$ Pa. When the deposition of Ti was performed with an EB evaporator, simultaneously, the pressure was decreased further to  $3.0 \times 10^{-3}$ Pa, satisfying stable operation of the ion source and the evaporator.

The ion energy can be varied between 5 to 25keV with nearly a constant beam current and the beam profile was a Gaussian with FWHM of 15-20mm. The increase of the substrate temperature by the beam injection to the sample was limited to about 500K in the energy range of the beam adopted.

Formation of  $TiO_2$  films was performed by varying the ion energy as well as the arrival rate  $Ti/O$  of Ti atoms and  $O^+$  ions onto Si single crystals and/or quartz plates. It was found that prepared films were all rutile type  $TiO_2$  crystals in contrast to amorphous or anatase type in other methods of  $TiO_2$  synthesis.

The growth of the crystal in the (110) plane was observed by increasing the ion energy and by decreasing the arrival rate. It was considered to be brought by the ion induced crystallization phenomenon characteristic to the ion beam technology and not by the temperature effect typically found in other methods.

From RBS analysis of prepared films it was found that the composition was stoichiometric with a ratio Ti:O of about 2, irrespective of the ion beam injection. This indicates the existence of a strong reactive process of Ti atoms on the film surface with the residual  $O_2$  molecules introduced from the ion source into the mixing chamber.

#### Acknowledgement

The authors would like to express their gratitudes to Dr. A. Chayahara, Government Industrial Research Institute, Osaka for his keen interest in this study, and to Dr. K. Takagi and Mr. A. Hoshino, ULVAC JAPAN, Ltd., for their support to the machine development and its modifica-

tion. They also thank to Mr. T. Usuki, Kinki University for his assistance in the experiment.

#### References

- 1) M. Satou, S. Fukui and F. Fujimoto, *Proc. 5th Symp. Ion Source and Ion-Assisted Technology, (Tokyo, 1981)* pp. 349.
- 2) M. satou, K. yamaguchi, Y. Andoh, Y. Suzuki, K. Matsuda and F. Fujimoto, *Nucl. Instrum & Methods* **B7/8**, 910 (1985).
- 3) M. Kiuchi, K. Fujii, T. Tanaka, M. Satou and F. Fujimoto, *Nucl. Instrum & Methods* **B33**, 649 (1988).
- 4) K. Ogata, Y. Andoh and E. Kamijo, *Nucl. Instrum. & Methods* **B39**, 178 (1989).
- 5) H. Oechsner, *Thin Solid Films* **175**, 119 (1989).
- 6) Y. Nakane, H. masuda, F. Fujimoto, Y. Honda, T. Miyazaki and S. Yano, *in 7th Int. Conf. on IBMM 90, Knoxville, Sept., 1990*.
- 7) S. Miyake, T. Kobayashi, M. Satou and F. Fujimoto, *Trans. of JWRI* **18**, 87 (1989).
- 8) H. Tsuboi, A. Hoshino and K. Takagi, *Proc. 13th Symp. on Ion Sources and Ion-Assisted Technology, Tokyo (1990)* p.17.
- 9) P. J. Martin, *J. Mat. Sci.* **21**, 1 (1986)
- 10) U. J. Gibson, *Phys. Thin Films* **13**, 87 (1987).
- 11) J. M. Bennett et al., *Appl. Optics* **28**, 3303 (1989).
- 12) K. Fukushima and I. Yamada, *J. Appl. Phys.* **65**, 619 (1989).
- 13) Y. Okabe, M. Iwaki, K. Takahashi, S. Ohira and B. U. Crist, *Nucl. Instrum & Methods* **B39**, 617 (1989).